

Contribution of electric quadrupole transitions to scattering cross section and collected current in a transmission electron microscope

Jean-Claude Le Bossé*

Université de Lyon, INSA-Lyon, MATEIS, UMR CNRS 5510, bat. B. Pascal, F-69621 Villeurbanne Cedex, France

(Received 19 October 2011; published 6 April 2012)

In this paper, the validity of the dipole approximation in the calculation of the double-differential scattering cross section (DDSCS) is investigated. A new expression of the DDSCS is obtained by adding to the classical term associated with the electric dipole transitions two terms taking the electric quadrupole transitions and the interference between dipole and quadrupole transition channels into account. In this study, we restrict to cases where the probed atom site is tetrahedral or octahedral. Moreover, the calculation of the average collected current (ACC) falling into the transition electron microscope collector is carried out by assuming that the incident electron beam is parallel. Then, DDSCS and ACC reduce to a linear combination of five intrinsic components, which only depend on the energy loss. The dominant intrinsic component is associated with the electric dipole transitions, three other intrinsic components are associated with the electric quadrupole transitions, and the last one, which cancels when the probed atom site is an inversion center, is associated with the interferences between dipole and quadrupole transition channels. These intrinsic components are rather hard to calculate, but their weights can be readily evaluated. In the case of the ACC, they essentially depend on the incident beam orientation and the collector aperture. The amplitudes of these weights allow us to evaluate the actual importance of the electric quadrupole transitions. At large collector aperture, the weights of the three quadrupole intrinsic components strongly increase and, thus, the contribution of the electric quadrupole transitions can not be neglected. At smaller collection angles, the importance of the electric quadrupole transitions can be estimated in each particular situation by comparing the amplitudes of the dipole and quadrupole intrinsic components.

DOI: [10.1103/PhysRevB.85.155112](https://doi.org/10.1103/PhysRevB.85.155112)

PACS number(s): 79.20.Uv

I. INTRODUCTION

The interpretation of electron energy loss near edge structure (ELNES) spectra requires the calculation of the double-differential scattering cross section (DDSCS).^{1–12} In order to have a good understanding of this quantity, let us imagine a fast electron in a state of wave vector \mathbf{k} and energy E moving to a target (see Fig. 1). The DDSCS is proportional to the number of fast electrons per unit of time, scattered into the solid angle $\delta\Omega$ located in the direction of the wave vector $\mathbf{k} + \mathbf{q}$, within an energy range δE centered at $E - \Delta E$. In the present case, we only consider scattered electrons which are involved in scattering events for which the energy loss ΔE of the fast incident electron is accompanied with the energy gain ΔE of an electron initially in a core atomic state of the target denoted by $|\varphi_i\rangle$. Then, this core electron is ejected to an unoccupied valence state of the target, denoted by $|\varphi_f\rangle$.

This event is only possible if ΔE is large enough to induce an electron transition to an *unoccupied* valence level ϵ_f located above the Fermi level. This event can be observed because it occurs just above the transition threshold associated with the particular core atomic level ϵ_i . Finally, the DDSCS is obtained by dividing the number per unit of time of these scattered electrons, by $\delta\Omega$, δE , and the number of fast incident electrons crossing a unit area during a unit of time. So, the DDSCS has the dimension of an area per unit of energy and per unit of solid angle.

The ELNES spectra collected in a transmission electron microscope (TEM) are obtained by measuring the current of electrons falling into a collector of solid angle $\Delta\Omega$ (see Fig. 1). Let us point out that the collector is aligned with the incident beam axis. Among the fast electrons, which have undergone an

energy loss ΔE , only a very small part of them are implicated into the excitation of a core electron of energy ϵ_i . However, the latter are revealed by a sudden increase of the collected current at the threshold energy. The contribution to the ELNES spectra of these electrons is obtained by subtracting the background due to the other inelastically scattered electrons. It is clear that an electron energy-loss spectroscopy (EELS) spectrum is proportional to the average of the DDSCS over the solid angle $\Delta\Omega$ of the collector. The acceptance cone of the detector is characterized by the collection semiangle β_m (see Fig. 1). The situation where β_m is about several times the characteristic angle θ_E given by

$$\theta_E = \frac{\Delta E \mathcal{E}_0}{\mathcal{E}_0^2 - m^2 c^4} \quad (1)$$

is a common situation. In the above expression of θ_E , $\mathcal{E}_0 = m\gamma c^2$ is the relativistic energy of the fast incident electron. The average of the DDSCS over an acceptance cone of several θ_E is often quite different from the DDSCS calculated for any direction of the transferred wave vector.^{13,14}

Let us note that the collection semiangle and the incident beam convergence angle are usually very small (≤ 50 mrad.). As a consequence, the modulus of the transferred wave vector q is small compared with the modulus of the incident wave vector k . On the other hand, the distance r from the core electron of energy ϵ_i to the atomic nucleus remains very small compared with the probed atom size. The scattering angle (denoted by β in Fig. 1), and thus the modulus q of the transferred wave vector, can be sufficiently small to make the dimensionless quantity $\mathbf{q} \cdot \mathbf{r} \ll 1$. In this case, the replacement of $\exp(i\mathbf{q} \cdot \mathbf{r})$ with its first-order expansion is a satisfactory approximation, called *dipole approximation*.^{15–21} It can be easily shown that

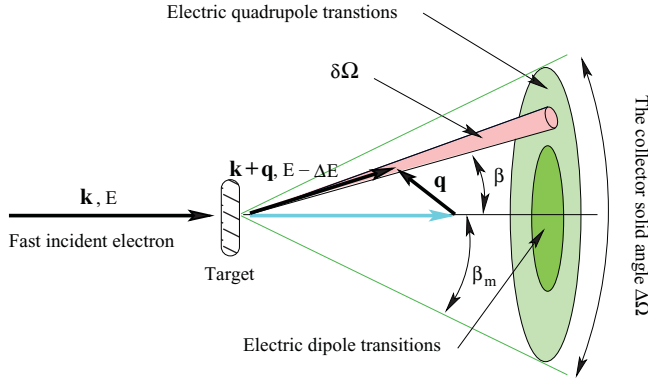


FIG. 1. (Color online) Double-differential scattering cross section and collected current of inelastically scattered electrons in a TEM.

if the scattering angle β is small, and if the energy loss ΔE is much smaller than the kinetic energy $\mathcal{E}_0 - mc^2$ of the fast incident electron, then q is approximately given by

$$q \approx \frac{1}{\hbar c} \sqrt{(\mathcal{E}_0^2 - m^2 c^4) \beta^2 + \frac{\mathcal{E}_0^2 \Delta E^2}{\mathcal{E}_0^2 - m^2 c^4}}. \quad (2)$$

In this expression,

$$\mathcal{E}_0^2 = \hbar^2 k^2 c^2 + m^2 c^4 \quad (3)$$

is the square of the relativistic energy of the fast incident electron. We can get some idea of the domain of validity of the dipole approximation by evaluating an upper bound of $\mathbf{q} \cdot \mathbf{r}$, that is to say of qr , at a distance r from the probed atom center for which the probability of finding the core electron is maximum. Actually, we have to consider $q \langle r \rangle$, in which $\langle r \rangle$ is the average distance from the core electron to the atomic nucleus, regardless of the direction of \mathbf{r} . This distance can be roughly estimated by assuming that the core electron wave function is a hydrogenlike radial wave function^{17,18} in which the nuclear charge Z has to be replaced with an effective nuclear charge Z^* , which takes the screening of the nucleus by other electrons into account. In any case, $Z^* < Z$ and thus keeping Z amounts to underestimate $q \langle r \rangle$. Other evaluations of $\langle r \rangle$ by using Slater-type orbitals or linear combinations of Slater-type orbitals^{22,23} lead to slightly larger values of $q \langle r \rangle$. So, use of these core wave functions leads to results very similar to those obtained by using hydrogenlike wave functions. We restrict here to K , L_{23} , and M_{45} edges for which the quantity $\langle r \rangle$ is given in Table I.

For the particular edges considered here (see caption of Fig. 2), it can be easily shown that for $\beta = \theta_E$, $q \langle r \rangle$ varies from 0.017 07 (case of the Rb M_{45} edge) to 0.0544 (case of the O K edge). So, the dipole approximation is indisputably valid for electrons collected near the collector center.²⁴ Figure 2

TABLE I. Average distance from a core electron to the probed atom center.

	K	L_{23}	M_{45}
Edge	$n_i = 1, \ell_i = 0$	$n_i = 2, \ell_i = 1$	$n_i = 3, \ell_i = 2$
$\langle r \rangle$	$3a_0/2Z$	$5a_0/Z$	$21a_0/2Z$

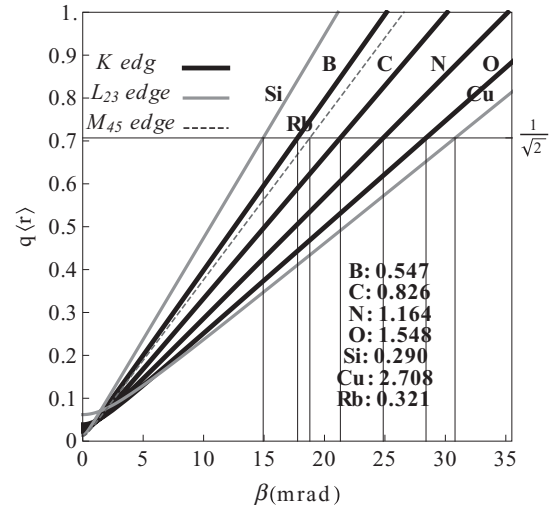


FIG. 2. This figure shows the variation of $q \langle r \rangle$ with the fast particle scattering angle [see Eq. (2)] β . Assuming that the incident electron beam energy is 200 keV, different edges are examined: B K edge, $\Delta E = 188$ eV, $Z = 5$; C K edge, $\Delta E = 284$ eV, $Z = 6$; N K edge, $\Delta E = 400$ eV, $Z = 7$; O K edge, $\Delta E = 532$ eV, $Z = 8$; Si L_{23} edge, $\Delta E = 99.2$ eV, $Z = 14$; Cu L_{23} edge, $\Delta E = 931$ eV, $Z = 29$; M_{45} Rb edge, $\Delta E = 110.3$ eV, $Z = 37$. For this incident beam energy, the value in mrad of the characteristic angle θ_E for each kind of probed atom is indicated.

shows that this approximation is obviously no longer valid when $\beta \gg \theta_E$. In the case of edges considered here, it can be observed that $q \langle r \rangle$ is $\sqrt{2}/2$ for scattering angles between 15 mrad (Si L_{23} edge) and 31 mrad (Cu L_{23} edge), a quite usual range for scattering angle β . Actually, if $q \langle r \rangle \gtrsim \sqrt{2}/2$, then it can be legitimately suspected that the second-order term, neglected in the dipole approximation, can introduce a non-negligible correction. Let us point out that the quantity $q \langle r \rangle \approx 1$ if β is 25 mrad for the boron and 35 mrad for the nitrogen. At these large scattering angles, it is clear that the dipole approximation is no longer valid. It will be shown that new scattering events involving *electric quadrupole transitions* from the atomic core levels takes place.²⁵

Let us recall that in the case where the dipole approximation is valid, the ELNES spectrum can be described as a linear combination of two (case of dichroism), three, four, or six (a , b , or c trichroism, respectively) particular DDSCS called *intrinsic components*.¹⁴ These different situations are related to the symmetry around the probed atom site, i.e., the site where the $|\varphi_i\rangle$ core atomic state is centered. Let us point out that an intrinsic component is DDSCS calculated when $\mathbf{q} = -\theta_E \mathbf{k}$ and a particular direction of \mathbf{k} . In this situation, the relativistic corrections disappear, and thus the intrinsic components can be obtained from a nonrelativistic computation.¹⁴ In the well-known case of dichroism, a threefold, fourfold, or sixfold rotation axis passes through the probed atom site. More precisely, an axial point group called *local group* completely describes the symmetry property of the probed atom site. In cases of trichroism, the local group is (1) or ($\bar{1}$) (c trichroism), (2) or (m) (b trichroism), ($2mm$) or (222) (a trichroism).^{14,26} In Sec. III B, it will be easily shown that the DDSCS in the dipole approximation is isotropic when the probed atom belongs to a

tetrahedral or an octahedral site. In these cases, the local point group may be (23), (m3), ($\bar{4}3m$) (432), or (m3m). They are the only cases where DDSCS and ELNES spectra can be directly compared. In any other case, the DDSCS is anisotropic, that is to say, it depends on the \mathbf{q} and \mathbf{k} directions, and thus ELNES spectrum and DDSCS may be very different.²⁷

This paper gives a treatment of the DDSCS which takes the contribution of the *electric quadrupole transitions* into account. With this treatment, the DDSCS is a sum of three terms: aside from the well-known term associated with the electron dipole transitions, there is a second term associated with the electron quadrupole transitions, and a third term taking the interference between dipole and quadrupole transition channels into account. The latter term cancels when the probed atom site is an inversion center. We restrict here to the situations where the probed atom site is tetrahedral or octahedral, for which the DDSCS under the dipole approximation is isotropic. In order to investigate the contribution to ELNES spectra of electric quadrupole transitions, the calculation of the current of inelastic scattered electrons collected in a TEM is required. For sake of simplicity, this calculation is restricted to the situation where the incident electron beam is parallel. As in the case of the dipole approximation,¹⁴ the collected current is a linear combination of intrinsic components associated with the three kinds of terms mentioned above. The relative importance of electric dipole and quadrupole transitions is governed by the relative weights of the dipole and quadrupole intrinsic components. Expressions of these weights, which essentially depend on the collection aperture and the incident beam energy, are given in the cases where the symmetry around the probed atom site is described with the five tetrahedral or octahedral point groups. As roughly shown in this section, this study establishes that the terms associated with quadrupole scattering events have a noticeable importance when the collection semiangle is much larger than the characteristic angle.

II. BEYOND THE DIPOLE APPROXIMATION

Many relativistic treatments of the DDSCS can be found in literature.^{13,14,28–31} The subsequent developments are actually based upon results obtained in Refs. 13, 14, and 30, which are gathered in Ref. 32. In the latter, it has been established that the general expression of the DDSCS is given by

$$\frac{\partial^2 \sigma}{\partial E \partial \Omega} = \frac{4\gamma^2}{a_0^2 q^4} \sum_{f \text{ unocc}} \left| \langle \varphi_f | \frac{\hat{O}}{1 - \frac{(\hat{\mathbf{q}} \cdot \mathbf{v})^2}{c^2}} | \varphi_i \rangle \right|^2 \delta(\epsilon_f - \epsilon_i - \Delta E). \quad (4)$$

In this expression, which is a sum over the unoccupied electron states labeled by f , $\hat{\mathbf{q}} = \frac{\mathbf{q}}{q}$ is the unit vector along the \mathbf{q} direction, and \mathbf{v} is the incident electron velocity

$$\mathbf{v} = \frac{\hbar \mathbf{k}}{m\gamma}, \quad (5)$$

which is related to the wave vector \mathbf{k} and the relativistic factor

$$\gamma = \frac{1}{\sqrt{1 - \frac{v^2}{c^2}}}. \quad (6)$$

The operator \hat{O} is given by

$$\hat{O} = e^{-i\mathbf{q} \cdot \mathbf{r}} + \frac{i\hbar e}{2mc^2} (\mathbf{v} \cdot \nabla e^{-i\mathbf{q} \cdot \mathbf{r}} + e^{-i\mathbf{q} \cdot \mathbf{r}} \mathbf{v} \cdot \nabla). \quad (7)$$

In Ref. 32, the theoretical developments have been carried out within the framework of the dipole approximation, based upon a first-order expansion in $\mathbf{q} \cdot \mathbf{r}$ of the operator \hat{O} . In this paper, we examine the contribution to the DDSCS of the second-order term.

A. Electric dipole, magnetic dipole, and electric quadrupole transitions

The expansion to the second-order of the operator \hat{O} leads to

$$\hat{O} = 1 - i\mathbf{q} \cdot \mathbf{r} + \frac{i\hbar}{mc^2} \mathbf{v} \cdot \nabla - \frac{1}{2} (\mathbf{q} \cdot \mathbf{r})^2 + \frac{\hbar}{2mc^2} ((\mathbf{v} \cdot \nabla)(\mathbf{q} \cdot \mathbf{r}) + (\mathbf{q} \cdot \mathbf{r})(\mathbf{v} \cdot \nabla)) + \dots \quad (8)$$

Let us emphasize that the symmetrical ordering of ∇ and \mathbf{r} in the last term of expression (8) must be preserved.³³ Using the identity³⁴

$$(\mathbf{q} \cdot \mathbf{r})(\mathbf{v} \cdot \nabla) = \frac{1}{2} [(\mathbf{q} \cdot \mathbf{r})(\mathbf{v} \cdot \nabla) + (\mathbf{v} \cdot \mathbf{r})(\mathbf{q} \cdot \nabla)] + \frac{1}{2} (\mathbf{q} \times \mathbf{v}) \cdot (\mathbf{r} \times \nabla) \quad (9)$$

and the relation

$$-i\hbar \nabla = \frac{m}{i\hbar} [\mathbf{r}, h_0]_- \quad (10)$$

in which h_0 is the Hamiltonian of the unperturbed system,³⁵ the expression (8) can be transformed into

$$\hat{O} = 1 - i \left(\mathbf{q} \cdot \mathbf{r} - \frac{1}{\hbar c^2} \mathbf{v} \cdot [\mathbf{r}, h_0]_- \right) + \frac{i}{2mc^2} (\mathbf{q} \times \mathbf{v}) \cdot \mathcal{L} - \frac{1}{2} (\mathbf{q} \cdot \mathbf{r})^2 + \frac{1}{2\hbar c^2} [(\mathbf{q} \cdot \mathbf{r})(\mathbf{v} \cdot \mathbf{r}), h_0]_- + \dots \quad (11)$$

In the above expression, $\mathbf{r} \times \nabla$ is expressed in terms of the orbital angular momentum $\mathcal{L} = -i\hbar \mathbf{r} \times \nabla$. Actually, the expression (11) is a sum of four terms.

(i) A zeroth-order term in $\mathbf{q} \cdot \mathbf{r}$, $\hat{O}^{(0)} = 1$.

(ii) A first-order term in $\mathbf{q} \cdot \mathbf{r}$. This term is associated with the *electric dipole transitions* and is given by

$$\hat{O}_{\text{ed}}^{(1)} = -i \left(\mathbf{q} \cdot \mathbf{r} - \frac{1}{\hbar c^2} \mathbf{v} \cdot [\mathbf{r}, h_0]_- \right). \quad (12)$$

(iii) A part of the second-order term in $\mathbf{q} \cdot \mathbf{r}$,

$$\hat{O}_{\text{md}}^{(2)} = \frac{i}{2mc^2} (\mathbf{q} \times \mathbf{v}) \cdot \mathcal{L}, \quad (13)$$

is associated with the *magnetic dipole transitions*. Its expression can be modified to take the electron spin \mathbf{S} into account. Then, we obtain

$$\hat{O}_{\text{md}}^{(2)} = \frac{i}{2mc^2} (\mathbf{q} \times \mathbf{v}) \cdot (\mathcal{L} + g\mathbf{S}) \quad (14)$$

instead of the expression (13). In the above expression, g is the Landé factor.

(iv) Another part of the second-order term in $\mathbf{q} \cdot \mathbf{r}$,

$$\hat{O}_{\text{eq}}^{(2)} = -\frac{1}{2}(\mathbf{q} \cdot \mathbf{r})^2 + \frac{1}{2\hbar c^2}[(\mathbf{q} \cdot \mathbf{r})(\mathbf{v} \cdot \mathbf{r}), h_0]_- \quad (15)$$

is associated with the *electric quadrupole transitions*. Let us note that the similar term encountered in x-ray absorption near-edge spectroscopy (XANES) is slightly different.²⁶ It is roughly obtained by removing the first term $-\frac{1}{2}(\mathbf{q} \cdot \mathbf{r})^2$, replacing \mathbf{q} with the polarization vector $\hat{\epsilon}$ of the electromagnetic field, and replacing \mathbf{v} with $\hbar\mathbf{k}/(m\gamma)$. In this way, if the dipole approximation becomes no longer valid, the XANES computation programs have to be used with circumspection for ELNES calculations.

B. Dipole and quadrupole matrix elements

The matrix element in the expression (4) of the DDSCS can be now evaluated. Assuming that the unoccupied valence state $|\varphi_f\rangle$ is orthogonal to the initial core state³⁶ $|\varphi_i\rangle$, this matrix element can be decomposed into

$$\begin{aligned} & \langle \varphi_f | \frac{\hat{O}}{1 - \frac{(\hat{\mathbf{q}} \cdot \mathbf{v})^2}{c^2}} | \varphi_i \rangle \\ &= \langle \varphi_f | \frac{\hat{O}_{\text{ed}}^{(1)}}{1 - \frac{(\hat{\mathbf{q}} \cdot \mathbf{v})^2}{c^2}} | \varphi_i \rangle + \langle \varphi_f | \frac{\hat{O}_{\text{md}}^{(2)}}{1 - \frac{(\hat{\mathbf{q}} \cdot \mathbf{v})^2}{c^2}} | \varphi_i \rangle \\ &+ \langle \varphi_f | \frac{\hat{O}_{\text{eq}}^{(2)}}{1 - \frac{(\hat{\mathbf{q}} \cdot \mathbf{v})^2}{c^2}} | \varphi_i \rangle + \dots \end{aligned}$$

1. Dipole matrix element

The first-order term is given by

$$\begin{aligned} \langle \varphi_f | \frac{\hat{O}_{\text{de}}^{(1)}}{1 - \frac{(\hat{\mathbf{q}} \cdot \mathbf{v})^2}{c^2}} | \varphi_i \rangle &= -i \langle \varphi_f | \frac{\mathbf{q} \cdot \mathbf{r} - \frac{1}{\hbar c^2} \mathbf{v} \cdot [\mathbf{r}, h_0]_-}{1 - \frac{(\hat{\mathbf{q}} \cdot \mathbf{v})^2}{c^2}} | \varphi_i \rangle \\ &= -i \langle \varphi_f | \frac{\mathbf{q} \cdot \mathbf{r} + \frac{\epsilon_f - \epsilon_i}{\hbar c^2} \mathbf{v} \cdot \mathbf{r}}{1 - \frac{(\hat{\mathbf{q}} \cdot \mathbf{v})^2}{c^2}} | \varphi_i \rangle. \end{aligned}$$

The presence of the Dirac distribution in (4) allows us to replace $\epsilon_f - \epsilon_i$ with the energy loss ΔE . Using the expression (1) of the characteristic angle and replacing \mathbf{v} with $\hbar\mathbf{k}/m\gamma$ lead to the new expression of the dipole matrix element

$$\langle \varphi_f | \frac{\hat{O}_{\text{de}}^{(1)}}{1 - \frac{(\hat{\mathbf{q}} \cdot \mathbf{v})^2}{c^2}} | \varphi_i \rangle = -i \langle \varphi_f | \mathbf{q}^* \cdot \mathbf{r} | \varphi_i \rangle \quad (16)$$

in which¹³

$$\mathbf{q}^* = \frac{\mathbf{q} + \frac{v^2}{c^2} \theta_E \mathbf{k}}{1 - \frac{v^2}{c^2} (\hat{\mathbf{q}} \cdot \hat{\mathbf{k}})^2}. \quad (17)$$

Let us remark the following:

(i) If $\frac{v}{c}$ approaches 0, then \mathbf{q}^* approaches \mathbf{q} . As a consequence, the nonrelativistic expression of the dipole matrix element is obtained by replacing \mathbf{q}^* with \mathbf{q} in (16).

(ii) If \mathbf{q} is parallel to \mathbf{k} , which means that $\mathbf{q} = -\theta_E \mathbf{k}$, then \mathbf{q} and \mathbf{q}^* coincide.

The last remark indicates that the relativistic corrections cancel when the scattering angle approaches 0. In the subsequent developments, we shall abundantly refer to this remark.

2. Magnetic dipole matrix element

The matrix element associated with magnetic dipole transitions is given by

$$\langle \varphi_f | \frac{\hat{O}_{\text{dm}}^{(2)}}{1 - \frac{(\hat{\mathbf{q}} \cdot \mathbf{v})^2}{c^2}} | \varphi_i \rangle = \frac{i}{2mc^2} \langle \varphi_f | \frac{(\mathbf{q} \times \mathbf{v}) \cdot (\mathcal{L} + g\mathbf{S})}{1 - \frac{(\hat{\mathbf{q}} \cdot \mathbf{v})^2}{c^2}} | \varphi_i \rangle. \quad (18)$$

Let us assume that the initial core electron state $|\varphi_i\rangle$ is characterized by a principal quantum number n_i , an azimuthal quantum number ℓ_i , a magnetic quantum number m_i , and a spin σ_i :

$$|\varphi_i\rangle = |n_i, \ell_i, m_i, \sigma_i\rangle. \quad (19)$$

According to the expression (18), the operator $\mathcal{L} + g\mathbf{S}$ acts on the core state $|n_i, \ell_i, m_i, \sigma_i\rangle$ and produces a linear combination of states $|n_i, \ell_i, m_i \pm 1, \sigma_i\rangle$ and $|n_i, \ell_i, m_i, \pm \frac{1}{2}\rangle$. In the present case where $\epsilon_i \lesssim -100$ eV, these bound states are orthogonal to the unoccupied valence states $|\varphi_f\rangle$. Therefore, the magnetic dipole matrix element cancels, which means that the magnetic dipole transitions do not participate in the ELNES spectra. A similar conclusion is obtained in the case of XANES.²⁶

3. Quadrupole matrix element

Its expression is given by

$$\begin{aligned} & \langle \varphi_f | \frac{\hat{O}_{\text{qe}}^{(2)}}{1 - \frac{(\hat{\mathbf{q}} \cdot \mathbf{v})^2}{c^2}} | \varphi_i \rangle \\ &= -\frac{1}{2} \langle \varphi_f | \frac{(\mathbf{q} \cdot \mathbf{r})^2 - \frac{1}{2\hbar c^2} [(\mathbf{q} \cdot \mathbf{r})(\mathbf{v} \cdot \mathbf{r}), h_0]_-}{1 - \frac{(\hat{\mathbf{q}} \cdot \mathbf{v})^2}{c^2}} | \varphi_i \rangle. \end{aligned}$$

Proceeding as in the case of the electric dipole matrix, we obtain

$$\langle \varphi_f | \frac{\hat{O}_{\text{qe}}^{(2)}}{1 - \frac{(\hat{\mathbf{q}} \cdot \mathbf{v})^2}{c^2}} | \varphi_i \rangle = -\frac{1}{2} \langle \varphi_f | (\mathbf{q} \cdot \mathbf{r})(\mathbf{q}^* \cdot \mathbf{r}) | \varphi_i \rangle. \quad (20)$$

As previously seen, the nonrelativistic expression of the electric quadrupole matrix element is obtained by replacing \mathbf{q}^* with \mathbf{q} .

Afterward, we shall consider the matrix element of the operator

$$\hat{a} = -i\mathbf{q}^* \cdot \mathbf{r} - \frac{1}{2}(\mathbf{q} \cdot \mathbf{r})(\mathbf{q}^* \cdot \mathbf{r}). \quad (21)$$

Neglecting the relativistic corrections ($\mathbf{q}^* = \mathbf{q}$), \hat{a} reduces to the sum of the first- and second-order terms obtained in the power-series expansion of $e^{i\mathbf{q}\mathbf{r}}$. In Appendix A, it is shown that a quadrupole electric transition from the initial state φ_i to a final state φ_f is governed by the *quadrupole selection rule*.

III. EXPRESSION OF THE DDSCS

A. Dipole, quadrupole transition channels and interferences between them

According to (21), the expression (4) of the DDSCS can be rewritten in the form

$$\frac{\partial^2 \sigma}{\partial E \partial \Omega} = \frac{4\gamma^2}{a_0^2 q^4} \sum_{f \text{ unocc}} |\langle \varphi_f | \hat{a} | \varphi_i \rangle|^2 \delta(\epsilon_f - \epsilon_i - \Delta E). \quad (22)$$

Replacing \hat{a} with its expression given in (21) leads to write the DDSCS in the form of a sum of three terms:

$$\frac{\partial^2 \sigma}{\partial \Omega \partial E} = \frac{\partial^2 \sigma^d}{\partial \Omega \partial E} + \frac{\partial^2 \sigma^{dq}}{\partial \Omega \partial E} + \frac{\partial^2 \sigma^q}{\partial \Omega \partial E}. \quad (23)$$

The first term is the dipole approximation of the DDSCS, and is given by

$$\frac{\partial^2 \sigma^d}{\partial E \partial \Omega} = \frac{4\gamma^2 q^{*2}}{a_0^2 q^4} \sum_{f \text{ unocc}} |\langle \varphi_f | \hat{\mathbf{q}}^* \cdot \mathbf{r} | \varphi_i \rangle|^2 \delta(\epsilon_f - \epsilon_i - \Delta E). \quad (24)$$

This term takes the electric dipole transitions into account. The third term is the quadrupole part of the DDSCS and is given by

$$\begin{aligned} \frac{\partial^2 \sigma^q}{\partial E \partial \Omega} &= \frac{\gamma^2 q^{*2}}{a_0^2 q^2} \sum_{f \text{ unocc}} |\langle \varphi_f | (\hat{\mathbf{q}} \cdot \mathbf{r})(\hat{\mathbf{q}}^* \cdot \mathbf{r}) | \varphi_i \rangle|^2 \\ &\times \delta(\epsilon_f - \epsilon_i - \Delta E). \end{aligned} \quad (25)$$

This term takes the electric quadrupole transitions into account. The second term describes the interferences between electric dipole and quadrupole transition channels. The contribution of interferences between these transition channels has already been investigated in the field of the photoelectron spectroscopy.^{37,38} This term is given by

$$\begin{aligned} \frac{\partial^2 \sigma^{qd}}{\partial E \partial \Omega} &= -\frac{4\gamma^2 q^{*2}}{a_0^2 q^3} \sum_{f \text{ unocc}} \text{Im}(\langle \varphi_f | \hat{\mathbf{q}}^* \cdot \mathbf{r} | \varphi_i \rangle \\ &\times \langle \varphi_i | (\hat{\mathbf{q}} \cdot \mathbf{r})(\hat{\mathbf{q}}^* \cdot \mathbf{r}) | \varphi_f \rangle) \delta(\epsilon_f - \epsilon_i - \Delta E). \end{aligned} \quad (26)$$

It must be noticed that, contrary to the dipole and quadrupole parts of the DDSCS, which are always strictly positive, the dipole quadrupole interference part of the DDSCS can be negative.

B. Dipole part of the DDSCS

1. Dipole intrinsic components

This part of the DDSCS is associated with electric dipole transitions for which the selection rule is $\Delta \ell = \pm 1$.³² Near a K edge ($\ell_i = 0$), an ELNES spectrum can be seen as a local p density of unoccupied states at the probed atom. The situation is a little more complicated near a L_{23} edge, where it would rather represent a mixture of local s and d densities of unoccupied states at the probed atom, and a term of interference between p to s and p to d transition channels.

It is very useful to separate the dependency on the orientation of the wave vectors \mathbf{q} and \mathbf{k} from the dependency on the variation of the energy loss ΔE near the transition edge. This separation can be easily carried out by rewriting the dipole DDSCS given in (24) as a quadratic form in the components \hat{q}_x^* , \hat{q}_y^* , and \hat{q}_z^* of the vector $\hat{\mathbf{q}}^* = \mathbf{q}^*/q^*$:

$$\frac{\partial^2 \sigma^d}{\partial E \partial \Omega} = \frac{q^{*2} q_{\min}^2}{q^4} \sum_{u,v} \hat{q}_u^* \hat{q}_v^* \Lambda_{uv}^d, \quad (27)$$

in which the coefficients Λ_{uv}^d given by

$$\Lambda_{uv}^d = \frac{4\gamma^2}{a_0^2 q_{\min}^2} \sum_{f \text{ unocc}} \langle \varphi_f | u | \varphi_i \rangle \langle \varphi_i | v | \varphi_f \rangle \delta(\epsilon_f - \epsilon_i - \Delta E) \quad (28)$$

have the dimension of a DDSCS. In the above expressions, u and v can take the values x , y , or z . The expression (28) does not depend on the directions of \mathbf{q} and \mathbf{q}^* , while it strongly depends on the variation of the energy loss ΔE . On the other hand, the factors $q_u^* q_v^* = q^{*2} \hat{q}_u^* \hat{q}_v^*$ in (27) weakly depend on the variations of ΔE as long as these variations remain small compared with ΔE , which is true for most ELNES spectra, while they strongly depend on the \mathbf{q} and \mathbf{q}^* orientations. By using the relations $\Lambda_{uv}^d = \overline{\Lambda_{vu}^d}$ obtained from (28), it can be seen that $\Lambda_{uv}^d + \Lambda_{vu}^d$ is real. Furthermore, for any pair of distinct labels u and v , we have the relation

$$\Lambda_{uv}^d + \Lambda_{vu}^d = \Lambda_{u+v, u+v}^d - \Lambda_{uu}^d - \Lambda_{vv}^d. \quad (29)$$

Then, the dipole part of the DDSCS can be rewritten in the form a linear combination of six *real* coefficients called intrinsic components¹⁴:

$$\begin{aligned} \frac{\partial^2 \sigma^d}{\partial E \partial \Omega} &= \frac{q_{\min}^2}{q^4} \{ q_x^* (q_x^* - q_y^* - q_z^*) \Lambda_{xx}^d + q_y^* (q_y^* - q_z^* - q_x^*) \\ &\times \Lambda_{yy}^d + q_z^* (q_z^* - q_x^* - q_y^*) \Lambda_{zz}^d + q_x^* q_y^* \Lambda_{x+y, x+y}^d \\ &+ q_y^* q_z^* \Lambda_{y+z, y+z}^d + q_z^* q_x^* \Lambda_{z+x, z+x}^d \}. \end{aligned} \quad (30)$$

It is the most general expression of the dipole part of the DDSCS, which is valid in the situation of (c) trichroism,¹⁴ when the local point group describing the symmetry of the probed atom site is (1) or ($\bar{1}$). For a higher symmetry around the probed atom site, the above expression can be markedly simplified. The dipole approximation of the DDSCS has been already evaluated for most of the probed atom site symmetries,¹⁴ and thus we shall not come back in detail to this problem. However, a much simpler method of finding most of the results of Ref. 14 is used here.³⁹ As this new method is applied to the investigation of the dipole quadrupole interference part and the quadrupole part of the DDSCS, it will be succinctly presented in the case of the dipole approximation. Here, we essentially focus on the cases of dichroism and isotropy.

2. Invariance of Λ_{uv}^d under any operation of the local group

The DDSCS must be unchanged under any operation of the local point group. For instance, in the case where this operation is a rotation by φ about the z axis, the transformation law of the coordinates is given by

$$(x, y, z) \rightarrow (x \cos \varphi - y \sin \varphi, x \sin \varphi + y \cos \varphi, z).$$

Note that this axis is henceforth chosen as the main rotation axis. In a more general case, any operation τ of the local point group is associated with a change of the u coordinate into

$$\tilde{u} = \sum_{u_1} \tau_{uu_1} u_1. \quad (31)$$

In this relation, τ is the usual matrix representation of the τ operation. In this way, the second-rank tensor Λ^d is

transformed into

$$\tilde{\Lambda}_{uv}^d = \sum_{u_1} \sum_{v_1} \tau_{uu_1} \tau_{vv_1} \Lambda_{u_1 v_1}^d. \quad (32)$$

As the dipole part of the DDSCS remains unchanged under any operation of the local point group, the matrix equation

$$\tilde{\Lambda}^d = \Lambda^d \quad (33)$$

must be satisfied. The number of independent matrix equations of this type is exactly the number of generators of the local point group.⁴⁰ A similar treatment can be carried out in the cases of third- and fourth-rank tensors appearing in the dipole quadrupole interference part and the quadrupole part of the DDSCS, respectively.

3. Case of dichroism

Let us examine the situation where the operation of the local group is a rotation of φ about the z axis. Using the property $\Lambda_{uv}^d = \overline{\Lambda_{vu}^d}$, the matrix equation (33) leads to

$$\sin \varphi [(\Lambda_{xx}^d - \Lambda_{yy}^d) \sin \varphi + (\Lambda_{xy}^d + \Lambda_{yx}^d) \cos \varphi] = 0, \quad (34a)$$

$$\sin \varphi [-(\Lambda_{xx}^d - \Lambda_{yy}^d) \cos \varphi + (\Lambda_{xy}^d + \Lambda_{yx}^d) \sin \varphi] = 0, \quad (34b)$$

$$\Lambda_{xz}^d (\cos \varphi - 1) - \Lambda_{yz}^d \sin \varphi = 0, \quad (34c)$$

$$\Lambda_{xz}^d \sin(\varphi) + \Lambda_{yz}^d (\cos \varphi - 1) = 0. \quad (34d)$$

As seen in Ref. 14, the case of b trichroism is obtained when $\varphi = \pi$. Then, the solution of these equations is $\Lambda_{xz}^d = \Lambda_{yz}^d = 0$ and the DDSCS is a linear combination of four intrinsic components. Restricting to cases where the probed atom belongs to a crystal, the angle φ can only take the remaining values $\frac{\pi}{3}$, $\frac{\pi}{2}$, $\frac{2\pi}{3}$. For these values, Eqs. (34c) and (34d) lead to $\Lambda_{xz}^d = \Lambda_{yz}^d = 0$, and Eqs. (34b) and (34c) lead to $\Lambda_{xx}^d - \Lambda_{yy}^d = 0$ and $\Lambda_{xy}^d + \Lambda_{yx}^d = 0$. By using these relations, it can be easily shown that (30) reduces to

$$\frac{\partial^2 \sigma^d}{\partial E \partial \Omega} = \frac{q_{\min}^2}{q^4} \{ (q_x^{*2} + q_y^{*2}) \Lambda_{xx}^d + q_z^{*2} \Lambda_{zz}^d \}, \quad (35)$$

which is the usual expression of the DDSCS in the case of dichroism. This expression is valid for any local point group except (i) the eight point groups of lower symmetry (1), ($\bar{1}$), (2), (m), ($2/m$), ($2mm$), (222), and (mmm); and (ii) the five point groups of higher symmetry (23), ($m3$), ($\bar{4}3m$), (432), and ($m3m$). For the 19 remaining axial point groups, no other generator than the rotation by $\frac{2\pi}{n}$ about the z axis can lead to a relation between the coefficients Λ_{uv}^d , which can modify the expression (35).

4. Cases where the local group is tetrahedral or octahedral

The five groups of higher symmetry have two common generators: a rotation by π about the Oz axis, and a rotation by $\frac{2\pi}{3}$ about the $[111]$ axis. These operations are associated with the coordinates transformations

$$(x, y, z) \rightarrow (-x, -y, z) \quad (36)$$

and

$$(x, y, z) \rightarrow (z, x, y), \quad (37)$$

respectively. As previously seen, the invariance under the first transformation leads to the relations $\Lambda_{xz}^d = \Lambda_{zy}^d = 0$. The second transformation leads to the relations $\Lambda_{xx}^d = \Lambda_{yy}^d = \Lambda_{zz}^d$ and $\Lambda_{xz}^d = \Lambda_{zy}^d = \Lambda_{yx}^d$. Use in expression (30) of these relations together with relation (29) leads to

$$\frac{\partial^2 \sigma^d}{\partial E \partial \Omega} = \frac{q^{*2} q_{\min}^2}{q^4} \Lambda_{xx}^d, \quad (38)$$

in which the intrinsic component Λ_{xx}^d is actually the dipole part of the DDSCS for any direction of $\mathbf{q} = -q_{\min} \hat{\mathbf{k}}$. The isotropy of the dipole part of the DDSCS when the probed atom site is tetrahedral or octahedral is a well-known result.

C. Dipole quadrupole interference part of the DDSCS

1. Intrinsic components

The expression (26) of the dipole quadrupole interference part of the DDSCS can be written as the cubic form

$$\frac{\partial^2 \sigma^{qd}}{\partial E \partial \Omega} = \frac{q_{\min}}{q^4} \sum_{u v w} q_u^* q_v q_w^* \Lambda_{u v w}^{qd} \quad (39)$$

in which

$$\Lambda_{u v w}^{qd} = -\frac{4\gamma^2}{a_0^2 q_{\min}} \sum_{f \text{ unocc}} \text{Im}(\langle \varphi_f | u | \varphi_i \rangle \langle \varphi_i | v w | \varphi_f \rangle) \times \delta(\epsilon_f - \epsilon_i - \Delta E). \quad (40)$$

The coefficients $\Lambda_{u v w}^{qd}$ depend on three labels u , v , and w , which can take the values x , y , or z . They have the dimension of a DDSCS and can be obtained from a nonrelativistic calculation. These coefficients can be considered as the intrinsic components of the dipole quadrupole interference part of the DDSCS. They only depend on the variation of the energy loss near the ionization threshold. On the other hand, the factor $q_{\min} q_u^* q_v q_w^* / q^4$ essentially depends on the orientation of the vectors \mathbf{q} and \mathbf{q}^* . In the case of a tetrahedral or an octahedral probed atom site, it may be at the origin of a DDSCS anisotropy. Let us remark that there are 6 distinct values of the matrix element $\langle \varphi_i | v w | \varphi_f \rangle$ and 3 distinct values of the matrix element $\langle \varphi_f | u | \varphi_i \rangle$. So, only 18 of the 27 coefficients $\Lambda_{u v w}^{qd}$ are distinct. From now, $\Lambda_{u v w}^{qd}$ is written with subscripts v and w in alphabetical order. Using the same notations as in Sec. III B2, the third-rank tensor Λ^{qd} is transformed into $\tilde{\Lambda}^{qd}$ under any operation τ of the local point group, and the invariance of the dipole quadrupole interference part of DDSCS under this operation is expressed by the matrix equation

$$\tilde{\Lambda}^{qd} = \Lambda^{qd}. \quad (41)$$

Let us remark that if the local point group contains the inversion of space, then

$$\tilde{\Lambda}_{u v w}^{qd} = -\Lambda_{u v w}^{qd} \quad (42)$$

and thus the above matrix equation leads to $\Lambda_{u v w}^{qd} = 0$. The dipole quadrupole interference part of the DDSCS cancels when the probed atom site is a center of inversion.

2. Cases where the local group is tetrahedral or octahedral

In this way, if the local point group is ($m\bar{3}$) (tetrahedral) or ($m\bar{3}m$) (octahedral), the dipole quadrupole interference part of the DDSCS cancels. A rotation by π about the z axis and a rotation by $\frac{2\pi}{3}$ about the [111] axis are two possible generators common to the three remaining point groups (23), ($\bar{4}3m$), and (432). The first rotation is associated with the coordinates transformation law given in (36). With this law, the matrix equation (41) leads to the cancellation of 10 of the 18 coefficients Λ_{uvvw}^{qd} , those for which the labels x and y appear once or three times in Λ_{uvvw}^{qd} :

$$\begin{aligned}\Lambda_{xxx}^{qd} &= \Lambda_{yyy}^{qd} = \Lambda_{yxx}^{qd} = \Lambda_{xyy}^{qd} = \Lambda_{xzz}^{qd} \\ &= \Lambda_{yzz}^{qd} = \Lambda_{xxy}^{qd} = \Lambda_{yyx}^{qd} = \Lambda_{zxx}^{qd} = \Lambda_{zyz}^{qd} = 0.\end{aligned}\quad (43)$$

The second rotation is associated with the coordinates transformation law (37). With this law, the matrix equation (41) leads to the cancellation of the five coefficients

$$\Lambda_{xxz}^{qd} = \Lambda_{yyz}^{qd} = \Lambda_{zzz}^{qd} = \Lambda_{zxx}^{qd} = \Lambda_{zyy}^{qd} = 0, \quad (44)$$

and the equality of the coefficients with three distinct labels

$$\Lambda_{zxy}^{qd} = \Lambda_{xzy}^{qd} = \Lambda_{yxz}^{qd}. \quad (45)$$

As a consequence, if the local point group is (23), the dipole quadrupole interference part of the DDSCS given in (39) reduces to the expression

$$\frac{\partial^2 \sigma^{qd}}{\partial E \partial \Omega} = \frac{2q_{\min}}{q^4} (q_z q_x^* q_y^* + q_x q_z^* q_y^* + q_y q_x^* q_z^*) \Lambda_{xyz}^{qd} \quad (46)$$

in which Λ_{xyz}^{qd} is obtained from the expression (40).

In the case where the local point group is ($\bar{4}3m$), the reflection in a vertical plane passing through the [110] axis is a possible third generator. It is associated with the coordinates transformation law

$$(x, y, z) \rightarrow (y, x, z). \quad (47)$$

The expression (46) of the dipole quadrupole interference part of the DDSCS is invariant under this transformation. Thus, this expression remains valid in the case where the local point group is ($\bar{4}3m$). If the local point group is (432) (the probed atom site is octahedral), there are three possible generators: a rotation by $\frac{2\pi}{3}$ about the [111] axis, a rotation by $\frac{\pi}{2}$ (instead of π in the cases of the two previous point groups) about the z axis, and a rotation by π about the [110] axis. The rotation by $\frac{\pi}{2}$ is associated with the following transformation of the coordinates:

$$(x, y, z) \rightarrow (-y, x, z). \quad (48)$$

In this case, the matrix equation (41) leads to the cancellation of 11 coefficients of the tensor Λ^{qd} :

$$\begin{aligned}\Lambda_{xxx}^{qd} &= \Lambda_{xxy}^{qd} = \Lambda_{xyx}^{qd} = \Lambda_{xzz}^{qd} = \Lambda_{yxx}^{qd} = \Lambda_{yxy}^{qd} \\ &= \Lambda_{yyx}^{qd} = \Lambda_{yzz}^{qd} = \Lambda_{zxx}^{qd} = \Lambda_{zyx}^{qd} = \Lambda_{zxy}^{qd} = 0,\end{aligned}\quad (49)$$

and the following relations:

$$\Lambda_{yxz}^{qd} = -\Lambda_{xyz}^{qd}, \quad \Lambda_{yzx}^{qd} = \Lambda_{xzx}^{qd}, \quad \Lambda_{zyy}^{qd} = \Lambda_{zxx}^{qd}. \quad (50)$$

These relations do not involve Λ_{zzz}^{qd} , and thus the dipole quadrupole interference part of the DDSCS depends at most on

four coefficients, as in the case where the local group is the (4) cyclic point group. The invariance of Λ^{qd} under the rotation by $\frac{2\pi}{3}$ leads to the cancellation of these four coefficients:

(i) Λ_{yxz}^{qd} , which is equal to $-\Lambda_{xyz}^{qd}$ [see Eq. (50)], is transformed into Λ_{xzy}^{qd} , and thus is zero;

(ii) Λ_{yyz}^{qd} is transformed into $\Lambda_{zxx}^{qd} = 0$ [see Eq. (49)];

(iii) Λ_{zyy}^{qd} is transformed into $\Lambda_{xzz}^{qd} = 0$ [see Eq. (49)];

(iv) Λ_{zzz}^{qd} is transformed into $\Lambda_{xxx}^{qd} = 0$ [see Eq. (49)].

It can be concluded that the dipole quadrupole interference part of the DDSCS cancels if the local point group is the (432), more precisely in any case where the probed atom site is octahedral. Finally, the dipole quadrupole interference part of the DDSCS is present only if the local point group is one of both tetrahedral groups (23) or ($\bar{4}3m$), and then its expression is given by (46).

D. Quadrupole part of the DDSCS

1. Quadrupole intrinsic components

This part is associated with the quadrupole electric transitions for which the selection rule is $\Delta\ell = 0, \pm 2$. Near a K edge, the part of ELNES spectra associated with the quadrupole electric transitions could be crudely interpreted as a picture of the s and d local density of unoccupied states at the probed atom. This interpretation is actually questionable because interferences between s to s and s to d transition channels can occur. The situation is even more complicated for L and M edges.

The expression (25) of the quadrupole part of the DDSCS can be rewritten as a quadrilinear form

$$\frac{\partial^2 \sigma^q}{\partial E \partial \Omega} = \frac{1}{q^4} \sum_{uvwt} q_u q_v^* q_w q_t^* \Lambda_{uvwt}^q \quad (51)$$

in which

$$\Lambda_{uvwt}^q = \frac{\gamma^2}{a_0^2} \sum_{f \text{ unocc}} \langle \varphi_f | uv | \varphi_i \rangle \langle \varphi_i | wt | \varphi_f \rangle \delta(\epsilon_f - \epsilon_i - \Delta E). \quad (52)$$

Note that the coefficients of the tensor Λ^q verify the relation

$$\overline{\Lambda}_{uvwt}^q = \Lambda_{wtuv}^q. \quad (53)$$

The expression (52) depends on four labels u, v, w , and t , which can take the values x, y , or z . So, the tensor Λ^q should depend on 81 coefficients. Actually, the expression (52) involves six distinct matrix elements $\langle \varphi_f | uv | \varphi_i \rangle$ and 6 other distinct matrix elements $\langle \varphi_i | wt | \varphi_f \rangle$. As a consequence, the tensor Λ^q , which might be represented as a 6×6 Hermitian matrix [see Eq. (53)], actually depends on 36 distinct coefficients instead of 81. Let us point out that both pairs (u, v) and (w, t) will be subsequently written in alphabetical order. Moreover, in expression (51), the factorization $q_u q_v^* q_w q_t^* (\Lambda_{uvwt}^q + \Lambda_{wtuv}^q)$ can be carried out. According to (53), the coefficients $\Lambda_{uvwt}^q + \Lambda_{wtuv}^q$ are real. So, for two distinct pairs of label, the off-diagonal coefficients of the 6×6 matrix mentioned above can be grouped together and, thus, the expression (51) involves a sum of $(6 \times 6 - 6)/2 = 15$ terms, which contain the real coefficients $\Lambda_{uvwt}^q + \overline{\Lambda}_{uvwt}^q$. Taking these terms and the diagonal elements of the form

$q_u q_v^* q_u q_v^* \Lambda_{uvuv}^q$ into account, the quadrupole part of the DDSCS reduces to a linear combination of 21 terms. It will be shown that the number of nonzero intrinsic components is markedly smaller in the case of a high symmetry around the probed atom site. Actually, the fourth-rank tensor Λ^q must be invariant under any generator of the local point group. As previously seen, the invariance of the quadrupole part of the DDSCS is expressed by a matrix equation of the form

$$\tilde{\Lambda}^q = \Lambda^q, \quad (54)$$

which leads to restrict the number of independent coefficients Λ_{uvwt}^q .

2. Cases where the local group is tetrahedral or octahedral

When the local group is one of the five point groups ($m3$), ($m3m$), (23), ($\bar{4}3m$), and (432), the quadrupole part of the DDSCS is at least invariant under a rotation by π about the z axis and a rotation by $\frac{2\pi}{3}$ about the [111] axis, that is to say under the coordinates transformations (36) and (37), respectively. The relation (54) applied to the case of the first rotation leads to the cancellation of 16 off-diagonal coefficients, those for which the labels x and y appear once or three times,

$$\begin{aligned} \Lambda_{xxxz}^q &= \Lambda_{xxyz}^q = \Lambda_{xyxz}^q = \Lambda_{xyyz}^q = \Lambda_{xzyy}^q = \Lambda_{xzzz}^q \\ &= \Lambda_{yyyz}^q = \Lambda_{yzzz}^q = 0, \end{aligned} \quad (55)$$

and their complex conjugates. The invariance of Λ^q under the transformation (37) leads to the cancellation of the four off-diagonal coefficients

$$\begin{aligned} \Lambda_{xxxy}^q &= \Lambda_{yyyz}^q = 0, \\ \Lambda_{xyyy}^q &= \Lambda_{yzzz}^q = 0, \\ \Lambda_{xyzz}^q &= \Lambda_{yzxx}^q = 0, \\ \Lambda_{xzyz}^q &= \Lambda_{xyxz}^q = 0, \end{aligned} \quad (56)$$

and their complex conjugates. Moreover, note the following:

(i) Six off-diagonal coefficients with two distinct labels verify the relations

$$\Lambda_{xxyy}^q + \Lambda_{yyxx}^q = \Lambda_{yyzz}^q + \Lambda_{zzyy}^q = \Lambda_{zzxx}^q + \Lambda_{xxzz}^q; \quad (57)$$

(ii) three diagonal coefficients with two distinct labels verify the relations

$$\Lambda_{xyxy}^q = \Lambda_{yzyz}^q = \Lambda_{xzxz}^q; \quad (58)$$

(iii) and three diagonal coefficients with one label verify the relations

$$\Lambda_{xxxx}^q = \Lambda_{yyyy}^q = \Lambda_{zzzz}^q. \quad (59)$$

So, expression (51) of the quadrupole part of the cross section, which now depends on three intrinsic components Λ_{xxx}^q , Λ_{xyxy}^q , and $\Lambda_{xyxy}^q + \Lambda_{yyxx}^q$, is transformed into

$$\begin{aligned} \frac{\partial^2 \sigma^q}{\partial E \partial \Omega} &= F_{xxxx}^q \Lambda_{xxx}^q + F_{xyxy}^q (\Lambda_{xyxy}^q + \bar{\Lambda}_{xyxy}^q) \\ &\quad + F_{xyxy}^q \Lambda_{xyxy}^q \end{aligned} \quad (60)$$

in which

$$F_{xxx}^q = \frac{q_x^2 q_x^{*2} + q_y^2 q_y^{*2} + q_z^2 q_z^{*2}}{q^4}, \quad (61a)$$

$$F_{xyxy}^q = \frac{q_x q_y q_x^* q_y^* + q_x q_z q_x^* q_z^* + q_y q_z q_y^* q_z^*}{q^4}, \quad (61b)$$

$$F_{xyxy}^q = \frac{(q_y q_x^* + q_x q_y^*)^2 + (q_z q_x^* + q_x q_z^*)^2 + (q_z q_y^* + q_y q_z^*)^2}{q^4}. \quad (61c)$$

The above expression is actually valid when the local point group is (23), the smallest of the five point groups of higher symmetry. If the local point group is ($m3$), then the inversion of space can be considered as a further generator. This operation amounts to change the sign of each coordinate. As Λ^q is unchanged under this transformation, the expression (60) remains valid in the case where the local group is ($m3$). The transition from the group (23) to the group ($\bar{4}3m$) is carried out by introducing a new generator, a reflection in a vertical plane containing the [110] axis. The coordinates transformation associated with this operation is given by (47). A permutation of coordinates x and y leaves the three relations (57), (58), and (59) unchanged. So, the expression (60) of the quadrupole part of the DDSCS remains valid in the case where the local group is ($\bar{4}3m$). The transition from the group (23) to the group (432) is carried out by replacing the rotation by π about the Oz axis with a rotation by $\frac{\pi}{2}$, and by considering a rotation of π about the [110] axis as a further generator. The invariance of Λ^q under these two new generators can be easily established by observing that the relations (57), (58), and (59) are unchanged when x is transformed into $\pm y$ and y is transformed into x . So, the expression (60) remains valid in the case where the local group is (432). The transition from (432) to the largest group ($m3m$) is obtained by introducing the inversion of space as a further generator. As previously seen, this new generator introduces no modification of relations (57), (58), and (59), and thus the expression (60) remains valid. Finally, when the local group is any of the five point groups of higher symmetry, i.e., when the probed atom site is tetrahedral or octahedral, the quadrupole part of the DDSCS can be calculated from the expressions (60) and (61).

IV. FROM THE DDSCS TO THE ELNES SPECTRUM

In the case of a parallel incident electron beam, an ELNES spectrum is the average of the DDSCS over a set of wave vectors for which the inelastically scattered electrons are collected. This section aims to calculate this average for scattered electrons which cause the ejection of an electron from a given core level.

A. Geometry of electron scattering

Let us assume that the probe is a cone-shaped incident electron beam. Its axis of revolution OZ , is oriented along the average incident wave vector \mathbf{k}_0 (see Fig. 3). The spatial coordinate system (X, Y, Z) and the basis vectors ($\mathbf{E}_x, \mathbf{E}_y, \mathbf{E}_z$) are tied to the incident electron beam, while the spatial coordinate system (x, y, z) and the basis vectors ($\mathbf{e}_x, \mathbf{e}_y, \mathbf{e}_z$) are tied to the sample. As previously mentioned, the Oz axis

in the case where the incident beam energy is 200 keV. If v_m approaches 0, the amplitude A_0 converges to 1, which expresses that ACC and DDSCS coincide when the collection semiangle approaches 0. Because of the DDSCS isotropy, the amplitude of the ACC does not depend on χ_0 and δ_0 , that is to say, on the incident beam orientation. The ACC strongly decreases near $v_m = 0$, and is approximately $2\Lambda_{xx}^d \ln(v_m)/v_m^2$ at large v_m . The amplitude A_0 will be a reference to test the importance of the dipole quadrupole interference part and the quadrupole part of the DDSCS.

C. Dipole quadrupole interference part of the collected current

Using the same conventions as in Sec. IV B, the evaluation of the dipole quadrupole interference part of the ACC is obtained by integrating the expression (46) over the collector solid angle. The calculation of this integral is rather tedious, and yet it can be easily carried out by using the MATHEMATICA software. The dipole quadrupole interference part of the ACC is given by the following expressions:

$$\left\langle \frac{\partial^2 \sigma^{qd}}{\partial E \partial \Omega} \right\rangle = E_0 \left\langle \frac{\partial^2 \sigma^{qd}}{\partial E \partial \Omega} \right\rangle_0, \quad (70a)$$

$$\left\langle \frac{\partial^2 \sigma^{qd}}{\partial E \partial \Omega} \right\rangle_0 = -3 \sin(2\delta_0) \sin^2(\chi_0) \cos \chi_0 \Lambda_{xyz}^{qd} \quad (70b)$$

$$E_0 = \frac{\gamma^2 + 4}{2(1 + \gamma^2 v_m^2)} - \frac{(\gamma^2 + 2) \ln(1 + \gamma^2 v_m^2)}{2\gamma^2 v_m^2}. \quad (70c)$$

Let us remark that the factor E_0 converges to 1 when the collection semiangle v_m approaches 0. In this way, $\langle \partial^2 \sigma^{qd} / \partial E \partial \Omega \rangle_0$ represents the limit of the dipole quadrupole interference part of the ACC when the collection semiangle approaches 0. Let us specify at this stage that the coordinate system used here is such that Ox , Oy , and Oz axes are the three twofold rotation axes of a regular tetrahedron, the summits of which are the four next-nearest-neighbor atoms of the probed atom (see the four spheres in Fig. 5). This

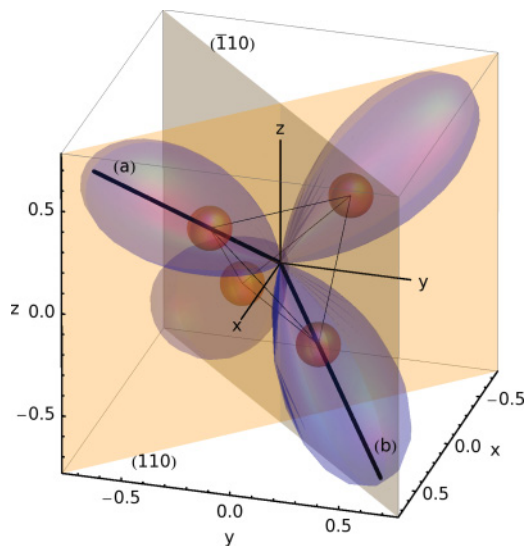


FIG. 5. (Color online) Amplitude of the dipole quadrupole interference part of the ACC as a function of the incident beam orientation.

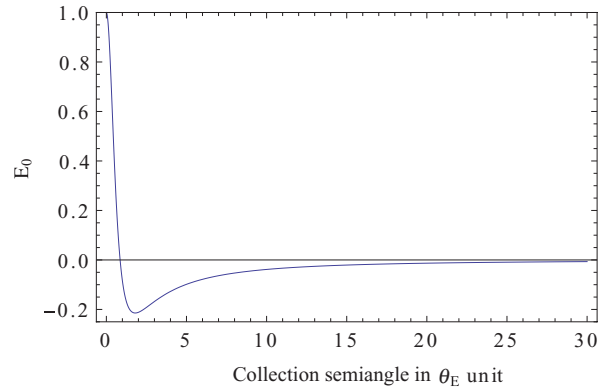


FIG. 6. (Color online) Amplitude E_0 of the dipole quadrupole interference part of the ACC versus the collection semiangle v_m .

figure shows the dependence on the incident electron beam orientation of the dipole quadrupole interference part of the ACC, when the collection semiangle is very close to 0. The amplitude of this factor is maximum in the plane (110), when the incident electron beam is oriented along the $[1\bar{1}1]$ direction [$\chi_0 \approx 54.73^\circ$ and $\delta = -45^\circ$, lobe (a)] and $[\bar{1}11]$ ($\chi_0 \approx 54.73^\circ$ and $\delta_0 = 135^\circ$). This amplitude is also maximum in the plane $(\bar{1}10)$, when the incident beam is oriented along the $[11\bar{1}]$ direction [$\chi_0 \approx 125.26^\circ$ and $\delta = 45^\circ$, lobe (b)] and $[\bar{1}\bar{1}\bar{1}]$ ($\chi_0 \approx 125.26^\circ$ and $\delta = 225^\circ$). The value of these maxima is $2\sqrt{3}$. So, a necessary condition to observe the dipole quadrupole interference part of the ACC is that the electron beam axis is oriented along one of the four directions shown in Fig. 5.

The relation (70a) indicates that the dipole quadrupole interference part of the ACC is proportional to a factor E_0 , which depends on γ and the collection semiangle v_m , in θ_E units [see (70c)]. Figure 6 shows its variations with v_m , when the electron beam energy is 200 keV. The factor E_0 decreases from 1 for $v_m = 0$ to about -0.214 for $v_m \approx 1.80$, then increases to 0 at larger collection semiangle. When the collection semiangle is approximately $0.86 \theta_E$, the amplitude E_0 cancels, which means that the dipole quadrupole interference part of the ACC vanishes. The importance of interferences between dipole and quadrupole channels can be truly investigated by examining the expression of the ACC. This expression, given by (68) in the case of the dipole approximation, becomes now

$$\left\langle \frac{\partial^2 \sigma}{\partial E \partial \Omega} \right\rangle = A_0 \left(\Lambda_{xx}^d - 3 \frac{E_0}{A_0} \sin(2\delta_0) \sin^2 \chi_0 \cos \chi_0 \Lambda_{xyz}^{qd} \right). \quad (71)$$

In the case of an incident electron beam of 200 keV, the ratio E_0/A_0 plotted in Fig. 7 decreases from 1 for $v_m = 0$ to $-(2 + \gamma^2)/(2\gamma^2) \approx -1.016$ as v_m approaches infinity. In the more favorable cases where the incident electron beam is oriented along one of the four directions for which $\langle \partial^2 \sigma^{qd} / \partial E \partial \Omega \rangle_0$ is maximum, the prefactor of Λ_{xyz}^{qd} in the expression (71) varies from -1.1547 for $v_m = 0$ to 1.1738 as v_m approaches infinity. So, at large collection semiangle, the weights of Λ_{xyz}^{qd} and Λ_{xx}^d have the same order of magnitude. It is widely accepted that the profile of an ELNES spectrum is mainly determined by the intrinsic component Λ_{xx}^d considered as a function of the energy loss ΔE . Interferences between transition channels

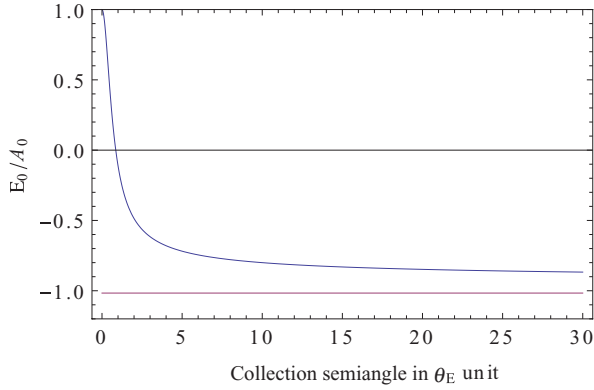


FIG. 7. (Color online) Ratio E_0/A_0 versus the collection semiangle v_m .

can be detected if this profile is noticeably affected by the introduction of the intrinsic component Λ_{xyz}^{qd} . So, in any particular situation where the local group is (23) or ($\bar{4}3m$), the comparison of both intrinsic components considered as functions of ΔE allows us to evaluate the importance of the interference between transition channels.

D. Quadrupole part of the collected current

According to (60), the quadrupole part of the ACC can be written as a sum three terms:

$$\left\langle \frac{\partial^2 \sigma^q}{\partial E \partial \Omega} \right\rangle = \left\langle \frac{\partial^2 \sigma_{xx xx}^q}{\partial E \partial \Omega} \right\rangle + \left\langle \frac{\partial^2 \sigma_{xx yy}^q}{\partial E \partial \Omega} \right\rangle + \left\langle \frac{\partial^2 \sigma_{xy xy}^q}{\partial E \partial \Omega} \right\rangle, \quad (72)$$

in which

$$\left\langle \frac{\partial^2 \sigma_{xx xx}^q}{\partial E \partial \Omega} \right\rangle = \frac{\Lambda_{xx xx}^q}{\pi v_m^2} \int_0^{2\pi} d\psi \int_0^{v_m} F_{xx xx}^q v dv, \quad (73a)$$

$$\left\langle \frac{\partial^2 \sigma_{xx yy}^q}{\partial E \partial \Omega} \right\rangle = \frac{\Lambda_{xx yy}^q + \overline{\Lambda}_{xx yy}^q}{\pi v_m^2} \int_0^{2\pi} d\psi \int_0^{v_m} F_{xx yy}^q v dv, \quad (73b)$$

$$\left\langle \frac{\partial^2 \sigma_{xy xy}^q}{\partial E \partial \Omega} \right\rangle = \frac{\Lambda_{xy xy}^q}{\pi v_m^2} \int_0^{2\pi} d\psi \int_0^{v_m} F_{xy xy}^q v dv. \quad (73c)$$

The calculation of the above integrals by using MATHEMATICA can be easily carried out. It leads to the following results:

$$\left\langle \frac{\partial^2 \sigma_{xx xx}^q}{\partial E \partial \Omega} \right\rangle = A_1 \Lambda_{xx xx}^q, \quad (74a)$$

$$\left\langle \frac{\partial^2 \sigma_{xx yy}^q}{\partial E \partial \Omega} \right\rangle = A_2 (\Lambda_{xx yy}^q + \overline{\Lambda}_{xx yy}^q), \quad (74b)$$

$$\left\langle \frac{\partial^2 \sigma_{xy xy}^q}{\partial E \partial \Omega} \right\rangle = A_3 \Lambda_{xy xy}^q, \quad (74c)$$

in which the weights A_i are given by

$$A_1 = B_1 + C_1 F, \quad (75a)$$

$$A_2 = B_2 + C_2 F, \quad (75b)$$

$$A_3 = B_3 + C_3 F, \quad (75c)$$

$$F = 8 \cos(4\delta_0) \sin^4 \chi_0 + 4 \cos(2\chi_0) + 7 \cos(4\chi_0). \quad (75d)$$

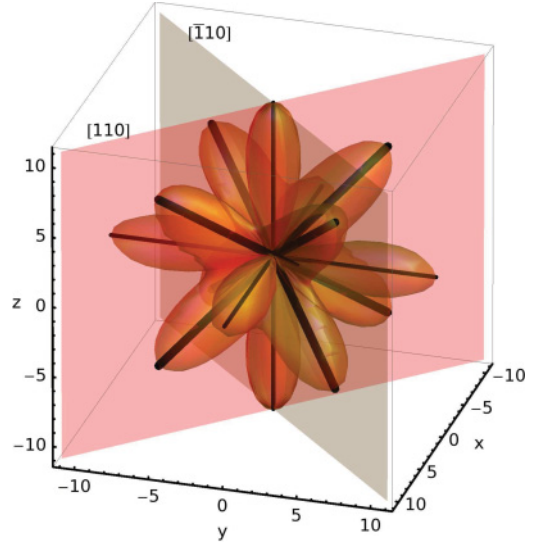


FIG. 8. (Color online) Anisotropy of the quadrupole part of the ACC associated with the incident beam orientation.

These weights are written in such a way that their dependency on the orientation of the fast incident wave vector \mathbf{k}_0 is separated from their dependency on the collection semiangle v_m . More precisely, the coefficients B_i and C_i only depend on the collector semiangle v_m and the relativistic factor γ , while the factor F only depends on χ_0 and δ_0 , i.e., the incident beam orientation. The factor F takes the anisotropy associated with the incident beam orientation into account, whereas the anisotropy associated with the orientation of the transferred wave vector \mathbf{q} comes from the other factors B_i and C_i . The calculation of B_i and C_i is rather tedious and the results of this calculation are reported in Appendix B.

The F factor is maximum when the incident beam is oriented along any of the three directions [100], [010], or [001]. In Fig. 8, these maxima correspond to six lobes of amplitude +11, identified by a thin line. This factor is minimum in any of the four directions [111], [$\bar{1}\bar{1}\bar{1}$], [$1\bar{1}\bar{1}$], or [$11\bar{1}$]. In Fig. 8, these minima correspond to the eight lobes of amplitude -10.33, identified by a thick line.⁴¹ The F factor cancels along many particular directions of the probe. For instance, in the azimuthal plane corresponding to $\delta_0 = \frac{\pi}{8}$, F cancels when $4 \cos 2\chi_0 + 7 \cos 4\chi_0 = 0$, that is to say, in the particular direction $\chi_0 \approx 27.33^\circ$. It can be concluded that the quadrupole part of the ACC strongly depends on the incident electron beam orientation.

According to expressions (72) and (74), the quadrupole part of the ACC is a linear combination of the three intrinsic components $\Lambda_{xx xx}^q$, $\Lambda_{xx yy}^q + \overline{\Lambda}_{xx yy}^q$, and $\Lambda_{xy xy}^q$. For a fixed direction of the incident electron beam, the weights of these components A_1 , A_2 , and A_3 , respectively, depend on the collector aperture. The contribution of the electric quadrupole transitions can be evaluated by examining the total ACC. If its dipole quadrupole interference part is neglected, the ACC is given by

$$\left\langle \frac{\partial^2 \sigma}{\partial \Omega \partial E} \right\rangle = A_0 \left(\Lambda_{xx}^d + \frac{A_1}{A_0} \Lambda_{xx xx}^q + \frac{A_2}{A_0} (\Lambda_{xx yy}^q + \overline{\Lambda}_{xx yy}^q) + \frac{A_3}{A_0} \Lambda_{xy xy}^q \right). \quad (76)$$

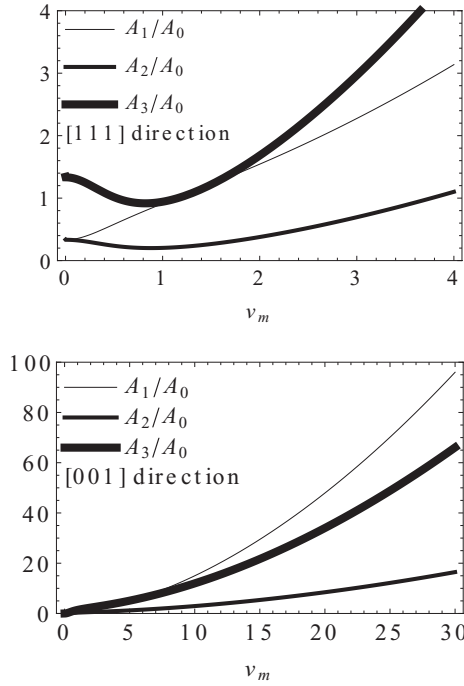


FIG. 9. Weights A_1/A_0 , A_2/A_0 , A_3/A_0 of the quadrupole intrinsic components $\Lambda_{xx,xx}^q$, $\Lambda_{xx,yy}^q$, and $\Lambda_{xy,xy}^q$ versus the collector semiangle, in the case where the probe is oriented along the [001] direction.

The importance of the quadrupole electric transitions can be investigated by comparing the amplitudes of the intrinsic components $\Lambda_{xx,xx}^q$, $\Lambda_{xx,yy}^q + \Lambda_{yy,xx}^q$ and $\Lambda_{xy,xy}^q$ to the amplitude of Λ_{xx}^d ; and by evaluating the ratios A_1/A_0 , A_2/A_0 , and A_3/A_0 at different collection semiangles. The first task, which depends on the particular probed atom and the solid at which it belongs, has to be carried out for any particular situation. We shall focus on the second task, which can be done in the general case.

For a fixed orientation of the incident electron beam, the anisotropy associated with the transferred wave-vector orientation is related to the variations of the weights A_1/A_0 , A_2/A_0 , and A_3/A_0 with the collection semiangle. Besides, changing the convergence of the incident beam,⁴² or equivalently the collection semiangle, is a possible approach to investigate the ELNES anisotropy. We are now going to consider the particular situation where the probe is oriented along the [001] direction.

For this probe orientation, the factor F is maximum. Let us first examine the case where the collector semiangle is lesser than $4\theta_E$. The top curve in Fig. 9 shows that if the collector semiangle is very small compared with θ_E ($v_m \ll 1$), the ratio $A_1/A_0 \simeq 1$ and both other ratios A_2/A_0 and A_3/A_0 cancel. As the weight $A_0 \simeq 1$ when $v_m \simeq 0$ (see Fig. 4), then the weight A_1 converges to 1 and both other weights A_2 and A_3 converge to 0. As a consequence, at very low collection semiangle, the quadrupole part of the ACC reduces to the intrinsic component $\Lambda_{xx,xx}^q$. This result can be easily explained by noting that if the incident beam is oriented along the [001] direction and the collector semiangle is very small compared with θ_E , then $\mathbf{q}^* = \mathbf{q}$ (see the remark at the end of Sec. II B 1), $q_z = q$, $q_x = q_y = 0$, and the components A_1 , A_2 , and A_3 converge to $F_{xx,xx}^q = 1$, $F_{xx,yy}^q + F_{yy,xx}^q = 0$, and $F_{xy,xy}^q = 0$,

respectively [see relations (61a), (61b), and (61c)]. Along the [100] or [010] directions of the incident electron beam, similar conclusions can be drawn.

In the case where the collection semiangle is no longer negligible compared with the characteristic angle θ_E , the weight A_1 of $\Lambda_{xx,xx}^q$ first decreases and has a minimum for $v_m \approx 0.8$, then increases for $v_m \gtrsim 0.8$, whereas both other weights, A_2 and A_3 , increase (see top curve in Fig. 9). Let us first note that, although \mathbf{k}_0 is oriented along the [001] direction, the dominant component in the quadrupole part of the ACC is no longer $\Lambda_{xx,xx}^q$ when $v_m \gtrsim 0.5$. As previously mentioned, the anisotropy associated with the orientation of the transferred wave vector is related to the variation of the ACC with the collection semiangle. For example, at very low aperture ($v_m \ll 1$), the quadrupole part of the ACC is about $\Lambda_{xx,xx}^q$ ($A_1/A_0 \approx 1$ and $A_2/A_0 = A_3/A_0 = 0$). The ELNES profile is partially determined by the dependency on the energy loss of $\Lambda_{xx,xx}^q$. If $v_m \approx 0.8$, then the quadrupole part of the ACC is about $0.66\Lambda_{xx,xx}^q + 0.26(\Lambda_{xx,yy}^q + \Lambda_{yy,xx}^q) + 1.165\Lambda_{xy,xy}^q$ and thus the profile of this quadrupole part is now predominantly determined by the dependency of $\Lambda_{xy,xy}^q$ on the energy loss. So, considering each of the intrinsic components as an independent function of the energy loss, the increase in the collector aperture does not only reduce to a change in the amplitude of this quadrupole part, but it also induces a change in its dependency on the energy loss.

This dependency on the \mathbf{q} orientation could be revealed in ELNES spectra if the three quadrupole intrinsic components were not too small compared with the dipole intrinsic component Λ_{xx}^d . Unfortunately, although the weights of $\Lambda_{xx,xx}^q$ and $\Lambda_{xy,xy}^q$ are, respectively, about 3 and 4 times the weight A_0 of Λ_{xx}^d for $v_m = 4$ (see top curves in Fig. 9), the above condition is not generally fulfilled in the low-aperture domain. In this domain, the profiles of ELNES spectra are essentially determined by the dipole intrinsic component Λ_{xx}^d , considered as a function of the energy loss ΔE . So, it can be concluded that if the collector semiangle $\beta_m \lesssim 4\theta_E$, the contribution to the ACC of the quadrupole electric transitions is generally negligible.

It can not be asserted that this conclusion remains valid when the collector semiangle $v_m \gg 1$. For $v_m \approx 30$, the bottom curve in Fig. 9 shows that the weights A_1 and A_3 are, respectively, about 70 and 100 times the weight A_0 of the dipole intrinsic component Λ_{xx}^d [see expression (76)]. Let us first note that for this collection semiangle, the weight A_1 of the intrinsic component $\Lambda_{xx,xx}^q$, which actually represents the quadrupole part of the DDSCS for $\mathbf{q} = -\theta_E \mathbf{k}_0$, is only 0.7 times the weight of the intrinsic component $\Lambda_{xy,xy}^q$. Let us also note that at large v_m , Fig. 9 roughly indicates that the ratios A_1/A_0 , A_2/A_0 , and A_3/A_0 proportionally increase, which prevents us to detect any dependency of the ACC on the transferred wave-vector orientation. For other orientations of the probe, similar conclusions can be drawn.

V. CONCLUSION

Our goal was to examine the validity of the dipole approximation in the theory of ELNES. We have been first led to consider the second-order expansion in $\mathbf{q} \cdot \mathbf{r}$ of the Hamiltonian, which describes the interaction between a fast

incident electron and an electron in a particular core state of the probed atom. Aside from the dipole matrix element, this expansion produces two further matrix elements associated with the magnetic dipole transitions and the electric quadrupole transitions. The first matrix element is absolutely negligible in the range of ionization energies commonly considered in ELNES. The second matrix element is different from the equivalent matrix element obtained in the absorption cross section calculated in XANES. If this element describes the transition from a core initial state of angular momentum ℓ_i to a final unoccupied state φ_f , it does not cancel only if the quadrupole selection rule is fulfilled. Then, the DDSCS can be decomposed into a sum of three terms: a first term associated with the electric dipole transition, a second term associated with the electric quadrupole transitions, and a third term that takes the interferences between both transition channels into account. This atypical third term cancels when the probed atom site is an inversion center. We have only considered here the cases of the five local point groups associated with a tetrahedral or an octahedral probed atom site. For these local groups, it has been easily shown that the dipole part of the DDSCS, which is proportional to one intrinsic component Λ_{xx}^d , is isotropic. It can be easily seen that the matrix element associated with the interference term is equal to zero when the local point group contains the inversion of space, which is the case when the local point group is $(m\bar{3})$ or $(m\bar{3}m)$. Although the point group (432) does not contain this operation, this matrix element is zero. In both remaining cases (23) and $(\bar{4}3m)$, the part of the DDSCS associated with interferences between transition channels is proportional to the intrinsic component Λ_{xyz}^{qd} . For all considered local point groups, the quadrupole part of the DDSCS is a linear combination of three intrinsic components Λ_{xx}^q , Λ_{yy}^q , and Λ_{xy}^q . It must be emphasized that the knowledge of the five intrinsic components allows us to calculate the DDSCS for any incident beam energy $\mathcal{E}_0 - mc^2$, any incident wave vector \mathbf{k} , and any scattered wave vector $\mathbf{k} + \mathbf{q}$.

Similarly, the collected current, i.e., the average of the DDSCS over the collector solid angle, is a linear combination of these five intrinsic components. Its dependence on the incident beam energy, the incident beam orientation, and the collection semiangle is entirely determined by the weights of these intrinsic components. Even if the collection semiangle β_m is large compared with the characteristic angle θ_E , the weights of the intrinsic components Λ_{xx}^d and Λ_{xyz}^{qd} have the same order of magnitude. So, in each particular situation where interferences between transition channels exist [(23) and $(\bar{4}3m)$], the importance of interferences between transition channels can be estimated by comparing the amplitudes of Λ_{xyz}^{dq} and Λ_{xx}^d . On the other hand, the larger the ratio $v_m = \beta_m/\theta_E$, the larger the weights of the quadrupole intrinsic components. When the collection semiangle β_m is larger than 30 times the characteristic angle θ_E , it has been verified for different beam orientations that these weights can reach or be larger than several hundred times the weight of the dipole intrinsic component. So, the quadrupole intrinsic components considered as functions of the energy loss ΔE can markedly modify the shape of the ELNES profile, even if these components are small compared with the dipole intrinsic

component. At lower collection semiangles, the importance of the quadrupole electric transitions can be estimated by comparing the three quadrupole intrinsic components with the dipole intrinsic component. Let us emphasize that, if these five intrinsic components are known, a simulation of the collected current as a function of the incident beam orientation and the collection semiangle can be carried out by using the weights given in Appendix A. All the previous conclusions remain true when the electron incident beam is not parallel.

APPENDIX A: THE QUADRUPOLE SELECTION RULE

The dimensionless quadrupole matrix element [see Eq. (20)]

$$a_{fi}^q = -\frac{1}{2} \langle \varphi_f | (\mathbf{q} \cdot \mathbf{r})(\mathbf{q}^* \cdot \mathbf{r}) | \varphi_i \rangle \quad (\text{A1})$$

can be evaluated by using the identity

$$\frac{1}{2} (\mathbf{q} \cdot \mathbf{r})(\mathbf{q}^* \cdot \mathbf{r}) = \frac{4\pi q q^* r^2}{15} \left(\frac{5}{8\pi} \hat{\mathbf{q}} \cdot \hat{\mathbf{q}}^* + \sum_{m=-2}^{+2} (-1)^m \mathcal{Y}_{2m}(\hat{\mathbf{q}}, \hat{\mathbf{q}}^*) Y_{2\bar{m}}(\hat{\mathbf{r}}) \right), \quad (\text{A2})$$

which allows us to express the above matrix element as a product of two factors. The first factor depends on the modulus q and q^* . The second factor depends on the orientation of \mathbf{q} and \mathbf{q}^* , i.e., on the unit vectors $\hat{\mathbf{q}}$ and $\hat{\mathbf{q}}^*$ along the direction of \mathbf{q} and \mathbf{q}^* , respectively. Let us point out that $-m$ is denoted by \bar{m} in expression (A2). The pseudospherical harmonics $\mathcal{Y}_{00}(\hat{\mathbf{q}}, \hat{\mathbf{q}}^*)$ and $\mathcal{Y}_{2m}(\hat{\mathbf{q}}, \hat{\mathbf{q}}^*)$ are given by

$$\begin{aligned} \mathcal{Y}_{00}(\hat{\mathbf{q}}, \hat{\mathbf{q}}^*) &= \sqrt{\frac{1}{4\pi}} (\hat{\mathbf{q}} \cdot \hat{\mathbf{q}}^*), \\ \mathcal{Y}_{22}(\hat{\mathbf{q}}, \hat{\mathbf{q}}^*) &= \sqrt{\frac{15}{32\pi}} (\hat{q}_x - i\hat{q}_y)(\hat{q}_x^* - i\hat{q}_y^*), \\ \mathcal{Y}_{21}(\hat{\mathbf{q}}, \hat{\mathbf{q}}^*) &= \sqrt{\frac{15}{32\pi}} [(\hat{q}_x - i\hat{q}_y)\hat{q}_z^* + (\hat{q}_x^* - i\hat{q}_y^*)\hat{q}_z], \\ \mathcal{Y}_{20}(\hat{\mathbf{q}}, \hat{\mathbf{q}}^*) &= -\sqrt{\frac{5}{16\pi}} (\hat{\mathbf{q}} \cdot \hat{\mathbf{q}}^* - 3\hat{q}_z\hat{q}_z^*), \end{aligned} \quad (\text{A3})$$

and their expressions for $m > 0$ are obtained by using the relation

$$\bar{\mathcal{Y}}_{2m}(\hat{\mathbf{q}}, \hat{\mathbf{q}}^*) = (-1)^m \mathcal{Y}_{2\bar{m}}(\hat{\mathbf{q}}, \hat{\mathbf{q}}^*). \quad (\text{A4})$$

Let us note that these pseudospherical harmonics reduce to the usual spherical harmonics when the relativistic corrections are neglected, that is to say, when $\mathbf{q}^* = \mathbf{q}$. The evaluation of the matrix element a_{fi}^q requires the knowledge of the initial and final wave functions $\varphi_i(\mathbf{r})$ and $\varphi_f(\mathbf{r})$. The initial core wave function

$$\varphi_i(\mathbf{r}) = R_{n_i \ell_i}(r) Y_{L_i}(\hat{\mathbf{r}}) \quad (\text{A5})$$

describes an electron in a core state characterized by the principal quantum number n_i and the pair of orbital quantum numbers $L_i = (\ell_i, m_i)$. The completeness relation between spherical harmonics³³ allows us to get the following

decomposition of the final wave function $\varphi_f(\mathbf{r})$ (Ref. 14):

$$\varphi_f(\mathbf{r}) = \sum_{L_1} R_{L_1}^{L_1}(f, r) Y_{L_1}(\hat{\mathbf{r}}). \quad (\text{A6})$$

Use of these wave functions leads to the following expression of $a_{f_i}^q$:

$$a_{f_i}^q = -\frac{4\pi q q^*}{15} \sum_{L_1} \Lambda_{L_1}^{qL_1}(\hat{\mathbf{q}}^*) \Upsilon_{L_1}^{qL_1}(f, n_i, \ell_i) \quad (\text{A7})$$

in which

$$\Upsilon_{L_1}^{qL_1}(f, n_i, \ell_i) = \int_0^\infty \bar{R}_{L_1}^{L_1}(f, r) R_{n_i \ell_i}(r) r^4 dr \quad (\text{A8})$$

and

$$\begin{aligned} \Lambda_{L_1}^{qL_1}(\hat{\mathbf{q}}^*) &= \frac{5}{\sqrt{16\pi}} \mathcal{Y}_{00}(\hat{\mathbf{q}}, \hat{\mathbf{q}}^*) \delta_{L_1 L_i} \\ &+ \sum_{m=-2}^{+2} (-1)^{m+m_1} C(L_1, 2\bar{m}, \bar{L}_1) \mathcal{Y}_{2m}(\hat{\mathbf{q}}, \hat{\mathbf{q}}^*). \end{aligned} \quad (\text{A9})$$

In this expression, the coefficients $C(L_1, L_2, L_3)$ are the well-known Gaunt coefficients. The expression (A7) indicates that an electron transition from the core state φ_i to a final state φ_f is only possible if $\Lambda_{L_1}^{qL_1} \neq 0$. It can be easily shown that this condition is fulfilled if $\ell_1 = \ell_i$ because of the first term of (A9). Use of the properties of the Gaunt coefficients⁴³ allows us to assert that the second term of (A9) does not cancel if

- (i) $m_1 = m_i - m$;
- (ii) $\ell_1 + \ell_i$ is even;
- (iii) $|\ell_i - 2| \leq \ell_1 \leq \ell_i + 2$.

These three conditions can be summarized into a simple rule called *quadrupole selection rule*:

$$\ell_1 = \ell_i \quad \text{or} \quad \ell_1 = \ell_i + 2 \quad \text{or} \quad \ell_1 = \max(0, \ell_i - 2). \quad (\text{A10})$$

A quadrupole electric transition from the initial state φ_i to a final state φ_f is possible only if the projection of the spherical harmonics Y_{L_1} onto the final state φ_f does not cancel when $\ell_1 = \ell_i$ or $\ell_1 = \ell_i \pm 2$.

APPENDIX B: B_i AND C_i COEFFICIENTS

The expressions of the prefactors A_1 , A_2 , and A_3 are rather complicated. They can be expressed in terms of the coefficients B_i and C_i given in Sec. IV D:

$$B_1 = \frac{159\gamma^4 v_m^2 - 2(22\gamma^4 - 155\gamma^2 + 22)}{256\gamma^2(1 + \gamma^2 v_m^2)} + \frac{(22\gamma^4 - 71\gamma^2 + 22) \ln(1 + \gamma^2 v_m^2)}{128\gamma^4 v_m^2}, \quad (\text{B1a})$$

$$C_1 = \frac{3\gamma^4 v_m^2 + 2(2\gamma^4 + 15\gamma^2 + 2)}{256\gamma^2(1 + \gamma^2 v_m^2)} - \frac{(2\gamma^4 + 11\gamma^2 + 2) \ln(1 + \gamma^2 v_m^2)}{128\gamma^4 v_m^2}, \quad (\text{B1b})$$

$$B_2 = \frac{97\gamma^4 v_m^2 + 44\gamma^4 - 54\gamma^2 + 44}{512\gamma^2(1 + \gamma^2 v_m^2)} - \frac{(22\gamma^4 - 71\gamma^2 + 22) \ln(1 + \gamma^2 v_m^2)}{256\gamma^4 v_m^2}, \quad (\text{B1c})$$

$$C_2 = -\frac{3\gamma^4 v_m^2 + 4\gamma^4 + 30\gamma^2 + 4}{512\gamma^2(1 + \gamma^2 v_m^2)} + \frac{(2\gamma^4 + 11\gamma^2 + 2) \ln(1 + \gamma^2 v_m^2)}{256\gamma^4 v_m^2}, \quad (\text{B1d})$$

$$B_3 = \frac{97\gamma^4 v_m^2 - 84\gamma^4 + 202\gamma^2 - 84}{128\gamma^2(1 + \gamma^2 v_m^2)} + \frac{3(14\gamma^4 - 19\gamma^2 + 14) \ln(1 + \gamma^2 v_m^2)}{64\gamma^4 v_m^2}, \quad (\text{B1e})$$

$$C_3 = -\frac{3\gamma^4 v_m^2 + 4\gamma^4 + 30\gamma^2 + 4}{128\gamma^2(1 + \gamma^2 v_m^2)} + \frac{(2\gamma^4 + 11\gamma^2 + 2) \ln(1 + \gamma^2 v_m^2)}{64\gamma^4 v_m^2}. \quad (\text{B1f})$$

The anisotropy of the ACC associated with the incident beam orientation comes from the dependency of F [see expressions (75)] on χ_0 and δ_0 . The anisotropy of the ACC associated with the transferred wave-vector orientation comes from the dependency on v_m of the above coefficients.

*jean-claude.lebosse@insa-lyon.fr

¹P. J. Durham, J. B. Pendry, and C. H. Hodges, *Comput. Phys. Commun.* **25**, 193 (1982).

²D. D. Vvedensky, D. K. Saldin, and J. B. Pendry, *Comput. Phys. Commun.* **40**, 421 (1986).

³D. K. Saldin, *Philos. Mag. B* **56**, 515 (1987).

⁴P. Rez, X. Weng, and H. Ma, *Microsc., Microanal., Microstruct.* **2**, 143 (1991).

⁵P. Rez, J. MacLaren, and D. K. Saldin, *Phys. Rev. B* **57**, 2621 (1998).

⁶M. Nelhiebel, P.-H. Louf, P. Schattschneider, P. Blaha, K. Schwarz, and B. Jouffrey, *Phys. Rev. B* **59**, 12807 (1999).

⁷A. L. Ankudinov, B. Ravel, J. J. Rehr, and S. D. Conradson, *Phys. Rev. B* **58**, 7565 (1998).

⁸P. Rez, J. R. Alvarez, and C. Pickard, *Ultramicroscopy* **78**, 175 (1999).

⁹P. Schattschneider, M. Nelhiebel, and B. Jouffrey, *Phys. Rev. B* **59**, 10959 (1999).

¹⁰A. L. Ankudinov and J. J. Rehr, *Phys. Rev. B* **62**, 2437 (2000).

¹¹J. Rusz, S. Rubino, and P. Schattschneider, *Phys. Rev. B* **75**, 214425 (2007).

¹²M. Moreno, K. Jorissen, and J. J. Rehr, *Micron* **38**, 1 (2007).

¹³J. C. Le Bossé, T. Épicier, and B. Jouffrey, *Ultramicroscopy* **106**, 449 (2006).

- ¹⁴J. C. Le Bossé, T. Épicier, and H. Chermette, *Phys. Rev. B* **76**, 075127 (2007).
- ¹⁵D. K. Saldin and J. M. Yao, *Phys. Rev. B* **41**, 52 (1990).
- ¹⁶D. K. Saldin and Y. Ueda, *Phys. Rev. B* **46**, 5100 (1992).
- ¹⁷Y. Ueda and D.K.Saldin, *Phys. Rev. B* **46**, 13697 (1992).
- ¹⁸R. F. Egerton, *Electron Energy-Loss Spectroscopy in the Electron Microscope*, 2nd ed. (Plenum, New York, 1996), pp. 230–233.
- ¹⁹M. P. Oxley and L. J. Allen, *Acta Crystallogr., Sect. A: Found. Crystallogr.* **56**, 470 (2000).
- ²⁰L. J. Allen, S. D. Findlay, M. P. Oxley, and C. J. Rossouw, *Ultramicroscopy* **96**, 47 (2003).
- ²¹C. Dwyer, *Ultramicroscopy* **104**, 141 (2005).
- ²²R. F. Egerton, *Ultramicroscopy* **4**, 169 (1979).
- ²³V. W. Maslen and C. J. Rossouw, *Philos. Mag. A* **47**, 119 (1983).
- ²⁴However, in the case where the incident beam convergence angle α_m is about 10 or more than 10 mrad, a fast incident electron with a large incidence angle can be scattered to the center of the collector with a large value of q .
- ²⁵J. M. Auerhammer and P. Rez, *Phys. Rev. B* **40**, 2024 (1989).
- ²⁶C. Brouder, *J. Phys.: Condens. Matter* **2**, 701 (1990).
- ²⁷V. Mauchamp, T. Épicier, and J. C. Le Bossé, *Phys. Rev. B* **77**, 235122 (2008).
- ²⁸U. Fano, *Phys. Rev.* **192**, 385 (1956).
- ²⁹C. Dwyer, *Phys. Rev. B* **72**, 144102 (2005).
- ³⁰P. Schattschneider, C. Hébert, H. Franco, and B. Jouffrey, *Phys. Rev. B* **72**, 045142 (2005).
- ³¹K. Jorissen, J. J. Rehr, and J. Verbeeck, *Phys. Rev. B* **81**, 155108 (2010).
- ³²P. Schattschneider, *Linear and Chiral Dichroism in the Electron Microscope* (Pan Stanford Publishing, Singapore, 2011).
- ³³C. Cohen-Tannoudji, *Quantum Mechanics*, Vol. 2 (Wiley, New York, 1977).
- ³⁴S. M. Blinder, *Foundation of Quantum Dynamics* (Academic, New York, 1971).
- ³⁵It is the system in which the interaction between incident and core electrons is switched off.
- ³⁶This is not necessarily true because φ_i is a one-electron eigenstate of the system with a Fermi filling of the states, while φ_f is a one-electron eigenstate of the system with a hole at the core energy level ϵ_i .
- ³⁷M. Krause, *Phys. Rev.* **177**, 151 (1969).
- ³⁸N. L. S. Martin, D. B. Thompson, R. P. Bauman, C. D. Caldwell, M. O. Krause, S. P. Frigo, and M. Wilson, *Phys. Rev. Lett.* **81**, 1199 (1998).
- ³⁹However, in cases where several transition channels exist (e.g., s and d channels for a L_{23} edge), this method does not allow us to express separately the contribution to the DDSCS of each transition channel and the interferences between them.
- ⁴⁰Let us assume that τ and σ are two generators of the point group. Let us denote by $\tilde{\Lambda}_\tau^d$ the transform under the operation τ of Λ^d [see Eq. (32)]. Then, it can be easily shown that if the equations $\tilde{\Lambda}_\tau^d = \Lambda^d$ and $\tilde{\Lambda}_\sigma^d = \Lambda^d$ are fulfilled, then the equation $\tilde{\Lambda}_{\sigma^q \cdot \tau^p}^d = \Lambda^d$ is fulfilled too. For any operation $a = \sigma^q \cdot \tau^p$ of the point group, the equation $\tilde{\Lambda}_a^d = \Lambda^d$ is fulfilled if the similar equations for the generators τ and σ of a are fulfilled.
- ⁴¹It does not mean that the collected current becomes negative. The weights $A_i = B_i + C_i F$ are always positive!
- ⁴²N. Browning, J. Yuan, and L. Brown, *Philos. Mag. A* **67**, 261 (1993).
- ⁴³P. M. Marcus and F. Jona, *Determination of Surface Structure by LEED* (Plenum, New York, 1984).